

Pressure-Driven Gas Flows in Micro Channels with a Slip Boundary: A Numerical Investigation

A. Aissa^{1, *}, M. E. A. Slimani², F. Mebarek-Oudina³, R. Fares¹, A. Zaim¹, L. Kolsi^{4, 5}, M. Sahnoun¹ and M. E. Ganaoui⁶

Abstract: In this paper, flow of slightly rarefied compressible nitrogen in microchannels has been investigated numerically for low values of Reynolds and Mach numbers. The 2D governing equations were solved using Finite Element Method with first-order slip boundary conditions (Comsol Multiphysics software). A validation was performed by comparing with similar configuration from the literature. It was found that our model can accurately predict the pressure driven flow in microchannels. Several interesting findings are reported about the Relative pressure, longitudinal velocity, Mach number, effect of gas rarefaction and flow rate.

Keywords: Pressure driven, slip flow, microchannels, gas flow, rarefaction effect.

1 Introduction

Gas flows in microsystems are of great importance and touch a variety of industrial fields; e.g., fluidic microactuators for active control of aerodynamic flows, micropumps, microvalves, micro-gas detectors, etc. [Fabricio, Mascouto, Naveira-Cotta et al. (2018); Barzegar Gerdroodbary, Ganji, Taeibi Rahni et al. (2018); Salimi and Mansourpanah (2017); Eid Mohamed (2016, 2017); Eid Mohamed and Mishra (2017); Eid Mohamed and Mahny (2017); Eid Mohamed, Mahny, Taseer et al. (2018); Wakif, Boulahia, Farhad et al. (2018); Eid Mohamed and Makinde (2018); Muhammad, Lu, Mahanthesh et al. (2018); Fares, Aissa, Meddeber et al. (2018)].

¹ Laboratoire de Physique Quantique de la Matière et Modélisation Mathématique (LPQ3M), University of Mascara, Mascara, Algeria.

² Department of Energetic and Fluid Mechanics, University of Science and Technology Houari Boumediene, Algiers, 16111, Algeria.

³ Department of Physics, Faculty of Sciences, University of 20 août 1955-Skikda, Skikda, Algeria.

⁴ Mechanical Engineering Department, College of Engineering, Haïl University, Haïl, 2240, Saudi Arabia.

⁵ Laboratory of Metrology and Energy Systems, University of Monastir, Monastir, 5000, Tunisia.

⁶ LERMAB, IUT Longwy, Université de Lorraine, Cosnes et Romain, 54400, France.

* Corresponding Author: A. Aissa. Email: aissa86@gmail.com.

Received: 23 July 2018; Accepted: 04 February 2020.

The study of macro and micro flows in microsystems can be performed basing on different approaches. The characteristic length scales that govern the energy and momentum transfer in MEMS (Micro-electro-mechanical systems) and their surrounding environments are in the order of microns. The need for understanding the behavior of rarefied flow in microsystems is an essential step for any technological application.

In such flows, various non-equilibrium transport phenomena appear. Thus the governing equations cannot be tackled by the typical Navier-Stokes approach. Under these rarefied conditions, the role played by the interactions between the gas and the solid device surface as well as in between the gas molecules become important. The boundary condition models often require empirical adjustments strongly depending on the (micro) manufacturing technique, while novel intermolecular collision models are subject to validation based on realistic potentials obtained by experimental works. The involved methodologies include extended hydrodynamics, kinetic theory and molecular dynamics [Valougeorgis, Vasileiadis and Titarev (2017); Pitakarnnop (2014)].

This division of the flow regimes is very important in order to choose the methods used for the modeling and prediction of the gas micro flows. Tab. 1 describes different regimes and governing equations of the gas micro flow depending on the Knudsen number, which is the key parameter to indicate the degree of rarefaction or state of non-equilibrium of gas flows [Aktas, Aluru and Ravailoi (2001)]. The Knudsen number can be defined as:

$$kn = \frac{\lambda}{h} \quad (1)$$

where λ is the mean free path and h , is the hole diameter.

The gas flow in microchannels can be treated in several ways such as the Direct Simulation Monte Carlo method (DSMC) [Aktas, Aluru and Ravailoi (2001); Bird (2006); Ameer, Croizet and Gatignol (2007); Hsieh, Tsai, Lin et al. (2004); Patsis, Ninos, Mathioulakis et al. (2013); Raza, Mebarek-Oudina and Mahanthesh (2019)]. Recently, the DSMC method has been applied to model the MEMS device. Note that the DSMC is a numerical method for modeling rarefied gas flows.

Table 1: Classification of gas flow regime [Hsieh, Tsai, Lin et al. (2004)]

Regime	Method of calculation	Kn range
Continuum flow	Navier-stokes and energy equation with no-slip boundary conditions	$Kn \leq 0.01$
Slip flow	Navier-stokes and energy equation with 0 slip boundary conditions	$0.01 < Kn \leq 0.1$
Transition flow	Boltzmann Transport equations, DSMC	$0.1 < Kn \leq 10$
Free molecule flow	Boltzmann Transport equations, DSMC	$Kn > 10$

Gas flow needs to be simulated using numerical models depending on the Knudsen number. But the rarefied gas cannot be modeled using classical CFD tools, due to the fact that kinetic effects are important due to the free path of the gas molecules that becomes comparable to the characterized length. The necessity of using models suited in every flow regime is well known [[Particle Tracing Module User's Guide](#)].

The prior researches which are similar to this work are those of Yang et al. [[Yang, Yang, Tai et al. \(1999\)](#)]; [Aktas, Aluru and Ravailoi \(2001\)](#); [Ameur, Croizet and Gatignol \(2007\)](#); [Gatignol \(2012\)](#)].

Yang et al. [[Yang, Yang, Tai et al. \(1999\)](#)] reported an experimental work carrying out the first experimental tests on a microfilter etched in a silicon wafer using the etching technique. Aktas et al. [[Aktas, Aluru and Ravailoi \(2001\)](#)] examined the flow of rarefied gases numerically in microchannel connects between two reservoirs using the multiscale method which is based on the Schwarz coupling of the DSMC coupled with Navier-Stokes equations.

Ameur et al. [[Ameur, Croizet and Gatignol \(2007\)](#)] carried out a numerical study of the gas flow in a microchannel with different geometries. Obtained results were compared with a solution of Poiseuille-Hagen flow. In contrast, an asymptotic model is proposed by Gatignol [[Gatignol \(2012\)](#)] to simulate isothermal gaseous flows in coplanar microchannel at low Mach numbers and with low to moderate Knudsen numbers. Burnett macroscopic equations for mass and momentum were written with slip conditions for velocity on the two micro-channel walls. Hsieh et al. [[Hsieh, Tsai, Lin et al. \(2004\)](#)] presented an experimental and theoretical study of low Reynolds number compressible gas flow (nitrogen) in a microchannel. Till now, all theoretical studies addressing compressible laminar flow remain insufficient to better describe the behavior of gases from the microfilter. In this study, a model that allows a fast solution for this type of flow is proposed.

This work is dedicated to the calculation of isothermal flow in microchannel. Numerical simulation using COMSOL code in the case of a Poiseuille type flow in slip regime is performed. Obtained results are used to validate the DSMC solution. This study is providing new information on the velocity profile and the pressure distribution.

2 Statement of the problem

For the present study, the nitrogen gas flow through a microchannel connects between two reservoirs [Fig. 1](#) is considered. The flow is created in the domain by the pressure gradients. The flow is directed from the left to the right pressure. P_{in} represents the pressure at the inlet of the first reservoir (1) and P_{out} is the pressure at the outlet of the second reservoir (2).

The gas pressures P_{in} , P_{out} and temperatures T at the two reservoirs, far from the connecting channel, are maintained constant with $P_{in} > P_{out}$. The walls of the reservoirs and of the channel are also maintained at temperature T . Due to the pressure difference there is an axisymmetric flow in the axial direction with the macroscopic distributions varying in the radial and axial directions [[Aktas, Aluru and Ravailoi \(2001\)](#)].

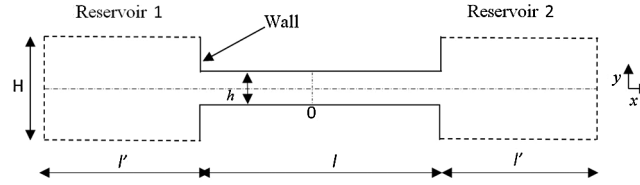


Figure 1: Description of the filter geometry studied in this work

2.1 Governing equations

The filter geometry shown in Fig. 1 was simulated with a CFD code. The proposed flow is two dimensional, steady, laminar and isothermal. The conservation equations system for the continuous approach of gaseous flows consists of two equations in partial derivatives expressing the mass and momentum conservation. The steady 2-D Navies-Stokes equations for a compressible fluid are written in the Cartesian coordinate system as:

The continuity equation:

$$\frac{\partial(\rho u_x)}{\partial x} + \frac{\partial(\rho u_y)}{\partial y} = 0 \quad (2)$$

The momentum conservation:

$$u_x \frac{\partial u_x}{\partial x} + u_y \frac{\partial u_x}{\partial y} = -\frac{1}{\rho} \frac{\partial p}{\partial x} + \nu \left(\frac{\partial^2 u_x}{\partial x^2} + \frac{\partial^2 u_x}{\partial y^2} \right) \quad (3)$$

$$u_x \frac{\partial u_y}{\partial x} + u_y \frac{\partial u_y}{\partial y} = -\frac{1}{\rho} \frac{\partial p}{\partial y} + \nu \left(\frac{\partial^2 u_y}{\partial x^2} + \frac{\partial^2 u_y}{\partial y^2} \right) \quad (4)$$

The equation of state for an ideal gas is given by:

$$p = \rho RT \quad (5)$$

where ρ and R are the density and the specific gas constant respectively.

The resolution of these partial differential equations requires the boundary conditions on the different borders of the study area [Gourari, Mebarek-Oudina, Hussein et al. (2019); Mebarek-Oudina and Bessaïh (2019)]. Boundary conditions in the walls are defined as functions of the Knudsen number.

- At the inlet (i.e., $x=-12 \mu\text{m}$); $P_1=P_{in}=1.3 \text{ atm}$
- At the outlet (i.e., $x=12 \mu\text{m}$); $P_2=P_{out}=1.0 \text{ atm}$

In the literature, the solution of the Navier-Stokes equations for the no-slip boundary condition at the wall is not applicable in the 'slip flow' regime. The momentum balance at the wall creates a no-slip velocity at the wall for gaseous flow. In this study, the

boundary condition reflecting a slip from the gas on the wall is used. It adopts the status of the first order for the velocity established by Maxwell [Maxwell (1879)]:

$$u_g - u_w = \lambda \frac{2 - a_v}{a_v} \frac{\partial u_g}{\partial y} \Big|_w \quad (6)$$

with

$$\lambda = \mu \sqrt{\frac{\pi}{2p\rho}} = \frac{\mu}{p} \sqrt{\frac{\pi r T}{2}} = \frac{\mu}{\rho} \sqrt{\frac{\pi}{2rT}} \quad (7)$$

where, u_w is the wall velocity u_g is the gas velocity, μ is the viscosity and ρ is the density.

Eq. (6), λ represents the local mean free path, a_v is the coefficient of accommodation for the momentum quantity.

Historically, flows in slip regime have been modeled by the direct simulation Monte Carlo (DSMC) method. This computes the trajectories of large numbers of randomized particles through the system but introduces statistical noise in modeling the process. For low velocity flows, such as those encountered in vacuum systems, the noise introduced by DSMC renders the simulations unfeasible. COMSOL uses alternative approaches: employing a discrete velocity method for transitional flows (using a Lattice Boltzmann velocity quadrature) and the angular coefficient method for molecular flows [Particle Tracing Module User's Guide].

Comsol allows to model slip flows and continuous medium. In the past, flows of these regimes were modeled using the direct simulation Monte Carlo (DSMC) method. It calculates the trajectories of a large number of random particles throughout the system but adds a statistical noise to the phenomena.

3 Computational grids

To assure the grid-independency of the present solution a mesh testing procedure was conducted. We examined nine different non-uniform grid systems with the following number of elements within the resolution field: 228, 524, 1148, 1912, 4174, 6792, 10550, 48216 and 181294. The numerical calculations is carried out by calculating the maximum velocity (v_{\max}) for the $x=0$ for said elements to develop an understanding of the grid fineness as shown in Tab. 2.

Table 2: Comparison of the maximum velocity V_{\max} for different grid resolutions

Grid number	228	524	1148	1912	4174	6792	10550	48216	181294
V_{\max} (m/s)	16.3	24.1	21.75	22.61	23.68	23.36	23.51	23.70	23.71

Tab. 2 shows that a grid size of 48216 elements is sufficient to obtain the grid independent solutions. In our numerical computation we have taken 48216 elements to obtain the grid independent solutions.

4 Results and discussion

In the present paper, two-dimensional pressure-driven gas flows through a microchannel is simulated in steady state. The flow is in the ‘slip flow’ regime, which is solved numerically using the slip velocity boundary condition. In the following, numerical and DSMC results are shown, compared and discussed.

Calculations were firstly performed for P_{in} as inlet pressure and P_{out} as outlet pressure at constant temperature of $T=300$ K and an imposed value for the accommodation coefficient ($a_v=1$).

Fig. 2 presents the different contours of the flow field parameters for nitrogen gas. The distribution of different flow field parameters in the microfilter domain are presented such as axial velocity, mean free path, Mach number, and pressure. This figure shows that the highest values of the Mach number are reached in the microchannel and this number is higher near to the exit, but it remains relatively small ($Ma < 0.1$).

The mean free path of the nitrogen gas throughout microfilter is illustrated on Fig. 2(b). Since the channel width is $1 \mu m$, a mean free path of 32 nm corresponds to a Knudsen number of 0.05 . This value is comparable to the Knudsen number of the gas in the channel the slip flow regime.

The pressure gradient is predominantly parallel to the walls. However, there are some normal pressure gradients in the vicinity of the opening of the channel, to be verified that the mean free path of gas molecule is proportional to the reciprocal of the pressure ($1/P$), so that the Knudsen number is proportional to $1/P$ as seen on the formula (5).

Fig. 3 shows the profile of the pressure along the axis ($y=0$) as a function of the micro-filament geometry. In all cases, an overpressure is observed at the upstream end of the micro-channel and. More the length of the inlet region is reduced more the gap between the pressure (P_{in}) and the pressure (P) increases. It was found that the pressure difference is lower in micro-filters. In addition, this difference in pressure is less important at the output compared to the input for all studied micro-channels. The upstream pressure has been noticed by Aktas et al. [Aktas, Aluru and Ravailoi (2001)], this is caused by the condition of reinjection of molecules in the computational domain at the level of the implementation of the so-called constant pressure condition.

Fig. 4 shows the evolution of the pressure along the micro-channel for different values of inlet pressure (P_{in}). Fig. 5, shows that the gradient of pressure in absolute value $\left(\frac{dp}{dx}\right)$ measured in $x=0$ increases gradually when the inlet pressure (P_{in}) grows. Note that the graph representing the absolute value $\left|\frac{dp}{dx}\right|$ for the pressure gradient by P_{in} is a line. The absolute value $\left|\frac{dp}{dx}\right|$ is therefore proportional to the inlet pressure.

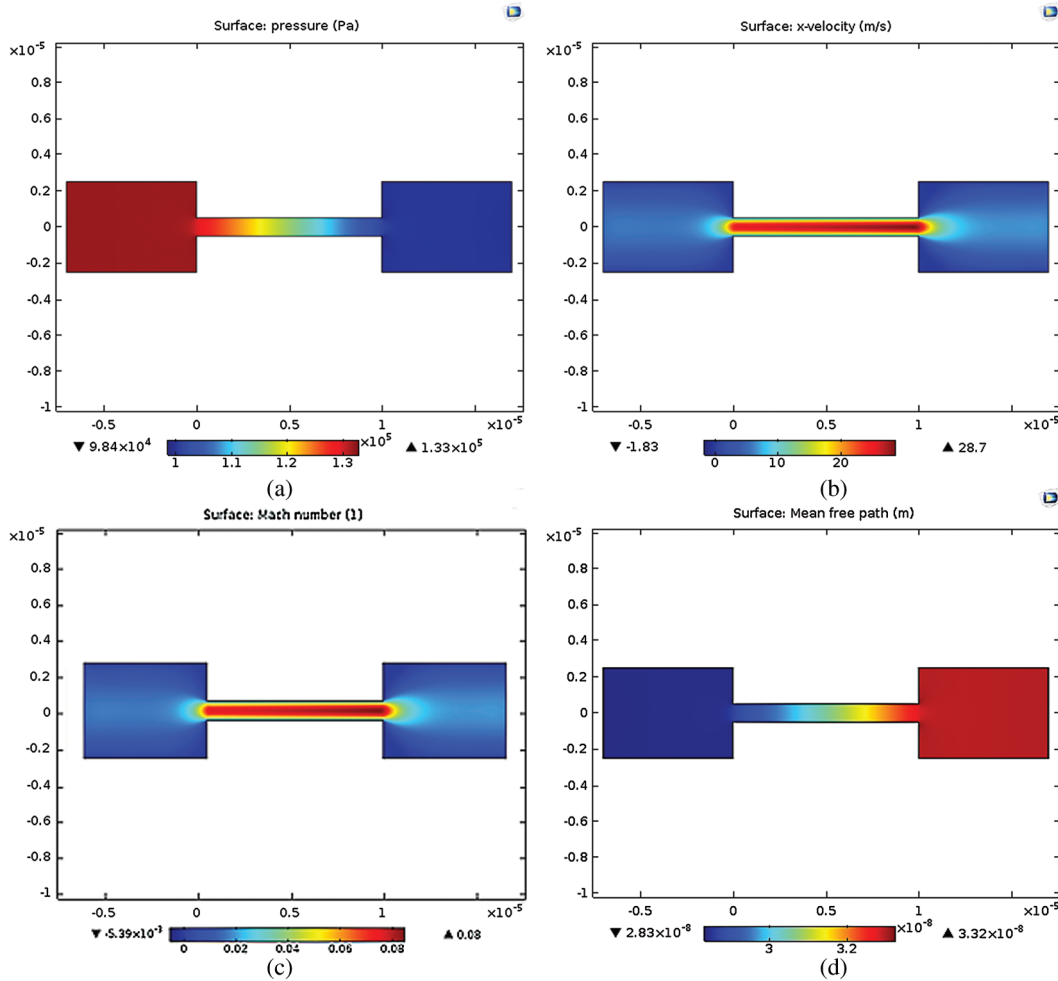


Figure 2: Fields of: (a) pressure, (b) x-velocity, (c) Mach number and (d) mean free path in microchannel

The comparisons between the numerical results and the DSMC solution are shown on Fig. 6. The variation of the pressure along the x-axis ($y=0$) obtained by numerical simulation with Comsol, DSMC [Gatignol (2012)] method developed by Bird [Bird (2006)] is presented. The domain of calculation is for a value of inlet pressure of $P_{in}=1.32$ kPa. This figure illustrates that there is a very good agreement between the two methods.

Fig. 6 shows the results for the average velocity of the gas, using two different models, i.e., the present model (Comsol), and DSMC models [Bird (2006)]. Excellent concordance between the present model and DSMC is observed,

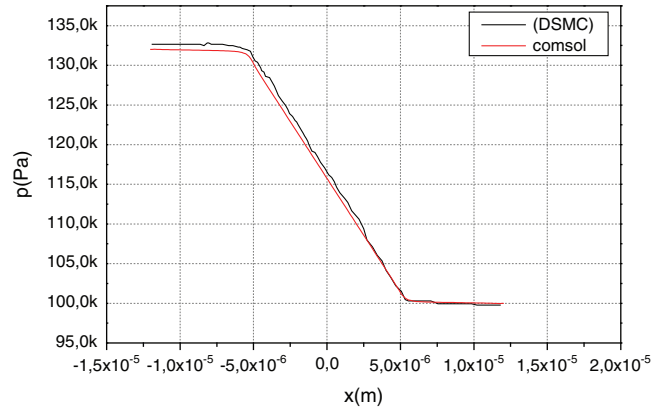


Figure 3: Pressure along the symmetry axis ($y=0$)

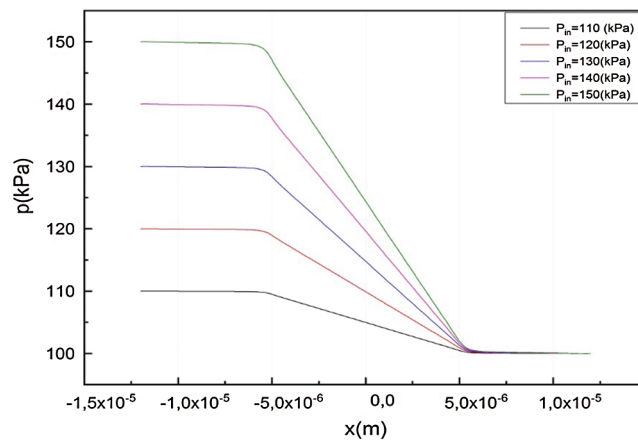


Figure 4: Relative pressure along the symmetry axis ($y=0$)

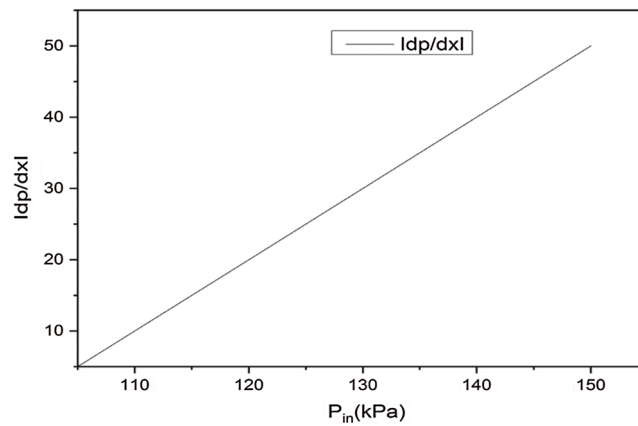


Figure 5: The absolute value of the pressure gradient measured on the symmetry axis of the micro-channel in $x=0$

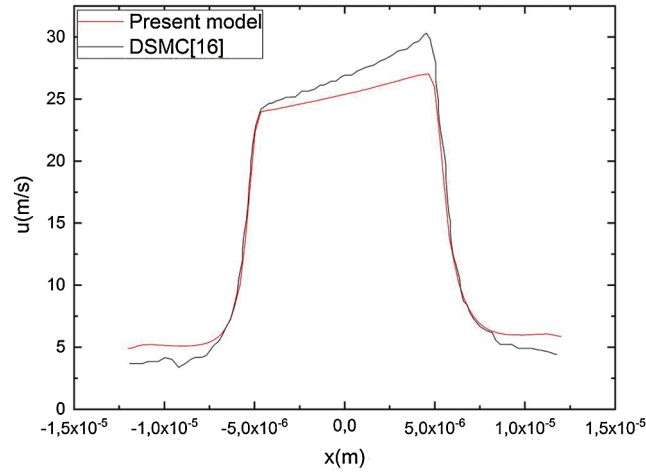


Figure 6: Longitudinal velocity along the $y=0$ axis

It should be noted that the values of the velocity x-component (u) are close for microchannel. However, it is found that this velocity is slightly higher when the length of the inlet chamber decreases. This can be understood by the increase in inlet pressure noted when the inlet length decreases.

From Fig. 7, it is noted that the value of the longitudinal velocity (for a fixed inlet pressure value P_{in}) is maximum near the exit of the microchannel. The example of the flow with an inlet pressure of 150 kPa and for a position x of 4.12×10^{-6} m, a velocity value of 40 m/s is obtained. In the entrance chamber, the longitudinal velocity is growing rapidly and continues to grow with a lower slope inside the micro-channel to its maximum value. At

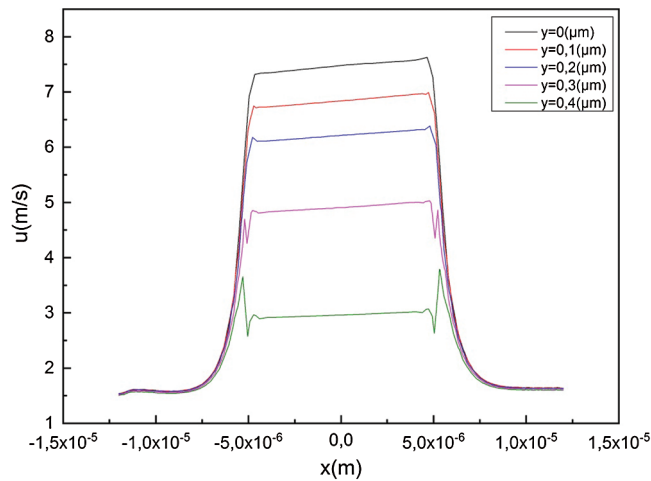


Figure 7: Longitudinal velocity along the axis of symmetry ($y=0$)

the outlet of the chamber, it decreases rapidly until its minimum value. For a fixed longitudinal position, the values of the velocity u increase when the value of the inlet pressure (P_{in}) is growing. The pressure increases in the inlet of the microchannel and decreases at the outlet.

Fig. 8 shows the profile of longitudinal velocities along the lines parallel to the axis of symmetry for an inlet pressure (P_{in}) of 1.1×10^5 Pa. This figure shows that there is a fluctuation at the inlet and the outlet of the microchannel at $y=0.5 \mu\text{m}$. This velocity fluctuation is due to the influence of the edges at the entrance and the exit.

Fig. 9 presents the profile obtained numerically with Comsol and the Poiseuille-Hagen [Ameur, Croizet, Maroteaux et al. (2008)] without slip and that of the numerical simulation obtained by the Monte-Carlo method (DSMC) [Gatignol (2012)].

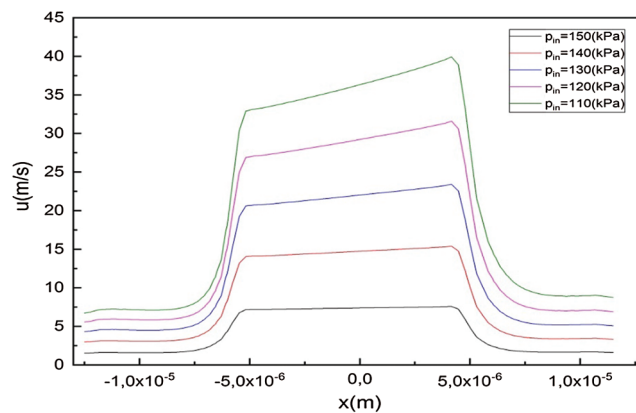


Figure 8: Longitudinal velocity along micro-channel for different lines of y

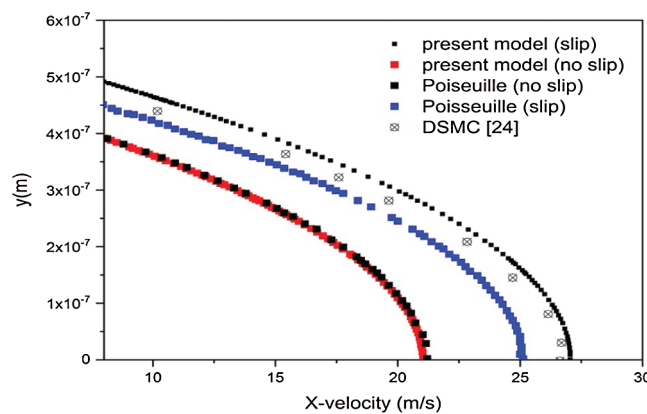


Figure 9: Velocity profiles u in the section $y=0$

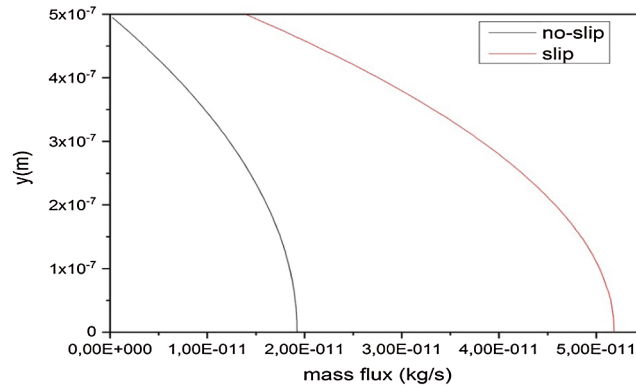


Figure 10: Nitrogen mass flow for $x=0$ in the micro-channel

The Poiseuille-Hagen solution using wall adhesion conditions gives a significant difference with the numerical solution. On the other hand, the comparison between the profiles resulting from the numerical computations and that of the sliding Poiseuille-Hagen flow shows a better agreement of the results Fig. 10. For all the different studied cases, these results are comparable. This highlights that the results have a greater agreement with the other methods, but the benefit of the present model is the calculation time (approximately 20 s) compared to DSMC that takes about 20 days.

5 Conclusions

In this paper, a numerical simulation was developed to investigate the pressure-driven of rarefied flow through the microchannel, by solving the Navier Stokes equations with slip condition at the wall using the first Maxwell. The flow in a microchannel in the 'slip flow' regime is simulated by the CFD code and compared with the DSMC method. The current results are compared with some available empirical formulations. The advantage of the present model is the very short calculation time compared to other models found in the literature. More work about the variation of non-dimensional pressure drop with opening factor will carry out in the future investigations.

Funding Statement: The author(s) received no specific funding for this study.

Conflicts of Interest: The authors declare that they have no conflicts of interest to report regarding the present study.

References

Aktas, O.; Aluru, N. R.; Ravailoi, U. (2001): Application of a parallel DSMC technique to predict flow characteristics in microfluidic filters. *Journal of Microelectromechanical Systems*, vol. 10, no. 4, pp. 538-549. DOI 10.1109/84.967377.

Ameur, D.; Croizet, C.; Maroteaux, F.; Gatignol, R. (2008): Simulation of pressure and temperature driven flows in microchannels. *AIP Conference Proceedings, Kyoto (Japan)*, pp. 1084-1129.

Ameur, D.; Croizet, C.; Gatignol, R. (2007): Microfilter flow modelling with DSMC method, LA HOUILLE BLANCHE/N° 06.

Bird, G. M. (2006). DSMC of Graeme Bird. <http://gab.com.au>.

Barzegar Gerdroodbary, M.; Ganji, D. D.; Taeibi Rahni, M.; Vakilipour, S. (2018): Effect of geometrical parameters on radiometric force in low-pressure MEMS gas actuator. *Microsystem Technologies*, vol. 24, no. 5, pp. 2189-2198. DOI 10.1007/s00542-017-3653-9.

Eid Mohamed, R. (2016): Chemical reaction effect on MHD boundary-layer flow of two-phase nanofluid model over an exponentially stretching sheet with a heat generation. *Journal of Molecular Liquids*, vol. 220, pp. 718-725. DOI 10.1016/j.molliq.2016.05.005.

Eid Mohamed, R. (2017): Time-dependent flow of water-NPs over a stretching sheet in a saturated porous medium in the stagnation-point region in the presence of chemical reaction. *Journal of Nanofluids*, vol. 6, no. 3, pp. 550-557. DOI 10.1166/jon.2017.1347.

Eid Mohamed, R.; Mishra, S. R. (2017): Exothermically reacting of non-Newtonian fluid flow over a permeable non-linear stretching vertical surface with heat and mass fluxes. *Computational Thermal Sciences*, vol. 9, no. 4, pp. 283-296. DOI 10.1615/ComputThermalScien.2017020298.

Eid Mohamed, R.; Mahny, K. L. (2017): Unsteady MHD heat and mass transfer of a non-Newtonian nanofluid flow of a two-phase model over a permeable stretching wall with heat generation/absorption. *Advanced Powder Technology*, vol. 28, no. 11, pp. 3063-3073. DOI 10.1016/j.appt.2017.09.021.

Eid Mohamed, R.; Mahny, K. L.; Taseer, M.; Sheikholeslami, M. (2018): Numerical treatment for Carreau nanofluid flow over a porous nonlinear stretching surface. *Results in Physics*, vol. 8, pp. 1185-1193. DOI 10.1016/j.rinp.2018.01.070.

Eid Mohamed, R.; Makinde, O. D. (2018): Solar radiation effect on a magneto nanofluid flow in a porous medium with chemically reactive species. *International Journal of Chemical Reactor Engineering*, vol. 7, pp. 201-212.

Fares, R.; Aissa, A.; Meddeber, M. A.; Aid Mohamed, A. (2018): Numerical investigation of hydrodynamic nanofluid convective flow in a porous enclosure. *Nature & Technology Journal*, vol. 18, pp. 54-57.

Fabricio, D. K.; Mascouto, S.; Naveira-Cotta, P.; Cotta, M. (2018): Conjugated heat transfer in circular microchannels with slip flow and axial diffusion effects. *International Communications in Heat and Mass Transfer*, vol. 91, pp. 225-233. DOI 10.1016/j.icheatmasstransfer.2017.12.003.

Hsieh, S. S.; Tsai, H. H.; Lin, C. Y.; Huang, C. F.; Chien, C. M. (2004): Gas flow in a long microchannel. *International Journal of Heat and Mass Transfer*, vol. 47, no. 17-18, pp. 3877-3887. DOI 10.1016/j.ijheatmasstransfer.2004.03.027.

- Gatignol, R.** (2012): Asymptotic modeling of flows in microchannel by using Navier-Stokes or Burnett equations and comparison with DSMC simulations. *Vacuum Journal*, vol. 86, no. 12, pp. 2014-2028. DOI 10.1016/j.vacuum.2012.04.043.
- Gourari, S.; Mebarek-Oudina, F.; Hussein, A. K.; Kolsi, L.; Hassen, W. et al.** (2019): Numerical study of natural convection between two coaxial inclined cylinders. *International Journal of Heat and Technology*, vol. 37, no. 3, pp. 779-786. DOI 10.18280/ijht.370314.
- James, R.** (2013): Molecular flow module: simulate rarefied gas flows in vacuum systems. www.comsol.com/blogs/molecular-flow-module-simulate-rarefied-gas-flows-in-vacuum-systems/.
- Maxwell, J. C.** (1879): On stresses in rarefied gases arising from inequalities of temperature. *Philosophical Transactions of the Royal Society of London*, vol. 170, pp. 231-256.
- Mebarek-Oudina, F.; Bessaïh, R.** (2019): Numerical simulation of natural convection heat transfer of copper-water nanofluid in a vertical cylindrical annulus with heat sources. *Thermophysics and Aeromechanics*, vol. 26, no. 3, pp. 325-334. DOI 10.1134/S0869864319030028.
- Pitakarnnop, J.** (2014): Rarefied gas flow in pressure and vacuum measurements. *Acta Imeko*, vol. 3, pp. 60-63.
- Patsis, G. P.; Ninos, K.; Mathioulakis, D.; Kaltsas, G.** (2013): Gas-mass-flow transfer-rate simulation and experimental evaluation in micro channels. *Microsystem Technologies Journal*, vol. 19, no. 12, pp. 1919-1925. DOI 10.1007/s00542-013-1763-6.
- Raza, J.; Mebarek-Oudina, F.; Mahanthesh, B.** (2019): Magnetohydrodynamic flow of nano williamson fluid generated by stretching plate with multiple slips. *Multidiscipline Modeling in Materials and Structures*, vol. 15, no. 5, pp. 871-894. DOI 10.1108/MMMS-11-2018-0183.
- Salimi, S.; Mansourpanah, Y.** (2017): Construction of a liquid droplet flowmeter for low-permeable gas separation membranes. *Journal of Membrane Science*, vol. 537, pp. 202-208. DOI 10.1016/j.memsci.2017.05.021.
- Muhammad, T.; Lu, D. C.; Mahanthesh, B.; Eid, M. R.; Ramzan, M.** (2018): Significance of Darcy-Forchheimer porous medium in nanofluid through carbon nanotubes. *Communications in Theoretical Physics*, vol. 70, no. 3, pp. 361-366. DOI 10.1088/0253-6102/70/3/361.
- Valougeorgis, D.; Vasileiadis, N.; Titarev, V.** (2017): Validity range of linear kinetic modeling in rarefied pressure driven single gas flows through circular capillaries. *European Journal of Mechanics-B/Fluids*, vol. 64, pp. 2-7. DOI 10.1016/j.euromechflu.2016.11.004.
- Wakif, A.; Boulahia, Z.; Farhad, A.; Eid Mohamed, R.; Sehaqui, R.** (2018): Numerical analysis of the unsteady natural convection MHD Couette nanofluid flow in the presence of thermal radiation using single and two-phase nanofluid models for Cu-water nanofluids. *International Journal of Applied and Computational Mathematics*, vol. 4, pp. 81.
- Yang, X.; Yang, J. M.; Tai, Y. C.; Ho, C. M.** (1999): Micromachined membrane particle filters. *Sensors Actuators Journal*, vol. 73, no. 1-2, pp. 184-191. DOI 10.1016/S0924-4247(98)00269-6.